1. Hau Huu VO[1], 2. Pavel BRANDSTETTER[2]

Ton Duc Thang University (1), VSB-Technical University of Ostrava (2)
ORCID: 1. 0000-0002-0904-307X; 2. 0000-0002-6742-7282

doi:10.15199/48.2023.11.30

Modified Fuzzy Logic PI Speed Controller with Scheduling Boundaries of Integral Time Constant for PMSM Drive

Abstract. *In order to obtain high performance speed response in pulse-width-modulation direct torque controlled drive of permanent magnet synchronous motor, fuzzy logic is utilized to update parameters of proportional-integral speed controller. However, overshoot and undershoot of speed response are still high, especially at times of load torque change. For reduction of the overshoot and undershoot, boundaries of integral time constant in fuzzy logic are tuned according to speed error during overshoot and undershoot. Theoretical assumptions are validated via simulations.*

Streszczenie. *Aby uzyskać wysoką wydajność odpowiedzi prędkości w sterowanym bezpośrednio momentem napędowym silnika synchronicznego z magnesami trwałymi z modulacją szerokości impulsu, do aktualizacji parametrów proporcjonalno-całkującego regulatora prędkości wykorzystywana jest logika rozmyta. Jednak przeregulowanie i niedoregulowanie odpowiedzi prędkości są nadal wysokie, zwłaszcza w okresach zmiany momentu obciążenia. W celu zmniejszenia przeregulowania i niedoregulowania, granice stałej czasowej całkowania w logice rozmytej są dostrajane zgodnie z błędem prędkości podczas przeregulowania i niedoregulowania. Założenia teoretyczne są weryfikowane za pomocą symulacji.* (*****Zmodyfikowany kontroler prędkości Fuzzy Logic PI z harmonogramem granic stałej czasowej całkowania dla napędu PMSM***)

Keywords: fuzzy logic, proportional-integral speed controller, integral time constant, direct torque control, permanent magnet synchronous motor.
Słowa kluczowe: logika rozmyta, proporcjonalno-całkujący regulator prędkości, stała czasowa całkowania, bezpośrednie sterowanie momentem obrotowym, silnik synchroniczny z magnesami trwałymi.

Introduction

Permanent Magnet Synchronous Motors (PMSMs) have been chosen in industrial applications such as electric vehicles, industrial robotics, tool machines, tower cranes because they provide low moment of inertia, high start-up torque, and high power [1, 2]. Besides field oriented control (FOC) strategy [3, 4], direct torque control (DTC) one with space vector pulse width modulation (SVPWM) technique has been utilized widely in motor torque control of both induction motor (IM) and PMSM drives [5, 6]. Intelligent control-based methods were effective solutions for speed controller in PMSM drives [7, 8, 9].

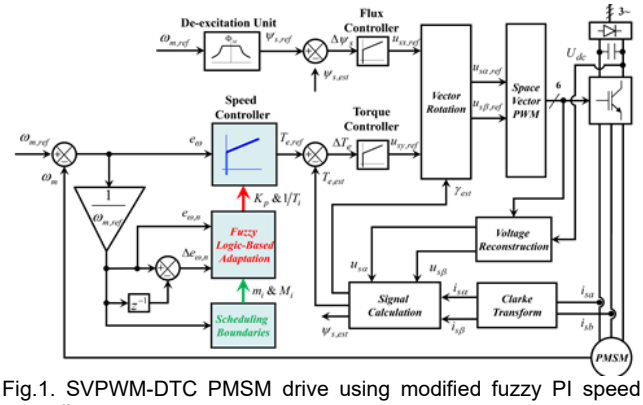

Fig.1. SVPWM-DTC PMSM drive using modified fuzzy PI speed controller

Among listed intelligent control methods, fuzzy logic was used to bring improved performance of system modelling, speed control, speed estimation for drives [10, 11, 12, 13, 14]. The fuzzy logic controller gave shorter response time for PMSM drive than proportional-integral (PI) one [10]. The fuzzy logic controller with reduced number of rule base, utilized inputs including motor torque error, position and error of stator flux to provide a desired voltage vector in sensorless IM drive [11]. Parameters of PI adaptation mechanism were adjusted by the fuzzy logic in sensorless IM drive [12]. Type-2 fuzzy logic was combined with hybrid duty ratio control to bring fast response with load torque or reference speed changes and lowered ripples of stator flux and motor torque [13]. The fuzzy logic was used in both approximation and optimal control of DC drive model [14]. In order to lower overshoot and undershoot of motor speed response, boundaries of integral time constant in fuzzy logic are proposed as linear functions of speed error.

Mathematical System Modelling

The SVPWM-DTC PMSM drive with fuzzy PI speed controller is shown in the Fig. 1. Mathematical PMSM model in stator coordinate system is expressed by Eqs. (1)-(6):

$$u_{s\alpha} = R_s i_{s\alpha} + \frac{d\psi_{s\alpha}}{dt} \tag{1}$$

$$u_{s\beta} = R_s i_{s\beta} + \frac{d\psi_{s\beta}}{dt} \tag{2}$$

$$\psi_{s\alpha} = L_s i_{s\alpha} + \psi_M \cos\theta_r \tag{3}$$

$$\psi_{s\beta} = L_s i_{s\beta} + \psi_M \sin\theta_r \tag{4}$$

$$T_e = 1.5\,p(i_{s\beta}\psi_{s\alpha} - i_{s\alpha}\psi_{s\beta}) \tag{5}$$

$$\frac{d\omega_m}{dt} = \frac{T_e - T_L}{J_m} \tag{6}$$

where: $u_{s\alpha}$, $u_{s\beta}$ – components of stator voltage; $\psi_{s\alpha}$, $\psi_{s\beta}$ – components of stator flux; $i_{s\alpha}$, $i_{s\beta}$ – components of stator current; θ_r – rotor position; R_s, L_s – stator resistance, *inductance*; ψ_M – PM magnetic flux; p – number of pole pairs; T_e – motor torque; T_L – load torque; ω_m – mechanical speed; J_m – motor inertia. List of PMSM parameters is shown in Table 1. Estimated values including stator flux components, stator flux magnitude, orienting angle, and motor torque, are computed by Signal Calculation block as follows:

$$\psi_{s\alpha,est} = \int \left(u_{s\alpha} - R_s i_{s\alpha}\right) dt \tag{7}$$

$$\psi_{s\beta,est} = \int \left(u_{s\beta} - R_s i_{s\beta}\right) dt \tag{8}$$

$$\psi_{s,est} = \sqrt{\psi_{s\alpha,est}^2 + \psi_{s\beta,est}^2} \tag{9}$$

$$\gamma_{est} = \arcsin\left(\psi_{s\beta,est} / \psi_{s,est}\right) \tag{10}$$

$$T_{e,est} = 1.5\,p\left(i_{s\beta}\psi_{s\alpha,est} - i_{s\alpha}\psi_{s\beta,est}\right) \tag{11}$$

Table 1. List of PMSM parameters [15]

Symbol	Quantity	Value
R_s	stator resistance	0.65 Ω
L_s	stator inductance	7.7 mH
ψ_M	magnetic flux of the PM	0.1706 Wb
p	number of pole pairs	4
P_N	nominal power	2.29 kW
n_N	nominal speed	3000 rpm @ f = 200 Hz
T_N	nominal torque	7.73 Nm
J_m	motor inertia	0.00151 kgm^2
U_{iRMS}	induced line-to-line voltage	263 V @ 3000 rpm
I_{SN}	nominal stator current	5.6 A

Speed Controller Utilizing Scheduled Fuzzy Logic Proportional-Integral Regulator

The PI speed controller (PISC) with fixed proportional gain K_p and integral time constant T_i (without blocks of Fuzzy Logic-Based Adaptation and Scheduling Boundaries) utilizes speed error e_ω to output reference motor torque $T_{e,ref}$ as follows:

$$T_{e,ref} = K_p\left(e_\omega + \frac{1}{T_i}\int_0^t e_\omega dt\right) \tag{12}$$

where $K_p > 0$, $T_i > 0$. Similar to observers [16], the $1/T_i$ parameter in Eq. (12) is ignored (see Eq. (13)) whenever reference motor torque $T_{e,ref}$ reaches $\pm T_N$ because this parameter has a greater influence on the performance of the speed control system than the K_p one.

$$T_{e,ref} = K_p e_\omega \tag{13}$$

The PISC is easy to implement but it does not guarantee the performance of the control system, especially at transient operations [12]. In order to improve the performance, the fuzzy logic is proposed to tune K_p, $1/T_i$. Next paragraph describes PI speed controller with Fuzzy Logic-Based Adaptation block (FL1SC).

At first, speed error e_ω is normalized by Eq. (14):

$$e_{\omega,n} = e_\omega / \omega_{ref} \tag{14}$$

where $e_{\omega,n}$ is limited in range ± 1. Linguistic variables of both normalized speed error $e_{\omega,n}$ and its difference $\Delta e_{\omega,n}$ have three values of $\{P, Z, N\}$, denoting for positive, zero, negative. Membership functions for $\{P, Z, N\}$ of $e_{\omega,n}$ and $\Delta e_{\omega,n}$ that are the $\Gamma-$, $\Lambda-$, $L-$ functions, are respectively described in Eqs. (15)-(17) and Eqs. (18)-(20):

$$\mu_P(e_{\omega,n}) = \begin{cases} 1, & e_{\omega,n} \ge B_e \\ \dfrac{e_{\omega,n}}{B_e}, & 0 \le e_{\omega,n} < B_e \\ 0, & e_{\omega,n} < 0 \end{cases} \tag{15}$$

$$\mu_Z(e_{\omega,n}) = \begin{cases} 0, & e_{\omega,n} \ge B_e \\ \dfrac{B_e - e_{\omega,n}}{B_e}, & 0 \le e_{\omega,n} < B_e \\ \dfrac{B_e + e_{\omega,n}}{B_e}, & -B_e \le e_{\omega,n} < 0 \\ 0, & e_{\omega,n} < -B_e \end{cases} \tag{16}$$

$$\mu_N(e_{\omega,n}) = \begin{cases} 0, & e_{\omega,n} \ge 0 \\ -\dfrac{e_{\omega,n}}{B_e}, & -B_e \le e_{\omega,n} < 0 \\ 1, & e_{\omega,n} < -B_e \end{cases} \tag{17}$$

$$\mu_P(\Delta e_{\omega,n}) = \begin{cases} 1, & e_{\omega,n} \ge B_e \\ \dfrac{\Delta e_{\omega,n}}{B_{\Delta e}}, & 0 \le \Delta e_{\omega,n} < B_{\Delta e} \\ 0, & \Delta e_{\omega,n} < 0 \end{cases} \tag{18}$$

$$\mu_Z(\Delta e_{\omega,n}) = \begin{cases} 0, & \Delta e_{\omega,n} \ge B_{\Delta e} \\ \dfrac{B_{\Delta e} - \Delta e_{\omega,n}}{B_{\Delta e}}, & 0 \le \Delta e_{\omega,n} < B_{\Delta e} \\ \dfrac{B_{\Delta e} + \Delta e_{\omega,n}}{B_{\Delta e}}, & -B_{\Delta e} \le \Delta e_{\omega,n} < 0 \\ 0, & \Delta e_{\omega,n} < -B_{\Delta e} \end{cases} \tag{19}$$

$$\mu_N(\Delta e_{\omega,n}) = \begin{cases} 0, & e_{\omega,n} \ge 0 \\ -\dfrac{\Delta e_{\omega,n}}{B_{\Delta e}}, & -B_{\Delta e} \le \Delta e_{\omega,n} < 0 \\ 1, & \Delta e_{\omega,n} < -B_{\Delta e} \end{cases} \tag{20}$$

where: B_e and $B_{\Delta e}$ are positive and selected experimentally. Fuzzy rule base which is shown in Table 2, utilizes two inputs $e_{\omega,n}$ and $\Delta e_{\omega,n}$ to output three linguistic values $\{L, M, S\}$ for K_p, $1/T_i$. The membership functions for $\{L, M, S\}$ are defined by Eqs. (21)-(26):

Table 2. Fuzzy rule base

$\Delta e_{\omega,n}$	$e_{\omega,n}$		
	P	Z	N
P	L, S	M, S	S, S
Z	L, M	M, M	S, M
N	L, L	M, L	S, L

$$\mu_L(K_p) = \begin{cases} 1, & K_p \ge M_p \\ \dfrac{K_p - med_p}{M_p - med_p}, & med_p < K_p < M_p \\ 0, & K_p \le med_p \end{cases} \tag{21}$$

$$\mu_M(K_p) = \begin{cases} 0, & K_p \le m_p \\ \dfrac{K_p - m_p}{med_p - m_p}, & m_p < K_p < med_p \\ \dfrac{M_p - K_p}{M_p - med_p}, & med_p \le K_p < M_p \\ 0, & K_p \ge M_p \end{cases} \tag{22}$$

$$\mu_S(K_p) = \begin{cases} 1, & K_p \le m_p \\ \dfrac{med_p - K_p}{med_p - m_p}, & m_p < K_p < med_p \\ 0, & K_p \ge med_p \end{cases} \tag{23}$$

$$\mu_L(T_i^{-1}) = \begin{cases} 1, & T_i^{-1} \ge M_i \\ \dfrac{T_i^{-1} - med_i}{M_i - med_i}, & med_i < T_i^{-1} < M_i \\ 0, & T_i^{-1} \le med_i \end{cases} \tag{24}$$

$$\mu_M(T_i^{-1}) = \begin{cases} 0, & T_i^{-1} \le m_p \\ \dfrac{T_i^{-1} - m_i}{med_i - m_i}, & m_i < T_i^{-1} < med_i \\ \dfrac{M_i - T_i^{-1}}{M_i - med_i}, & med_i \le T_i^{-1} < M_i \\ 0, & T_i^{-1} \ge M_i \end{cases} \tag{25}$$

$$\mu_S(T_i^{-1}) = \begin{cases} 1, & T_i^{-1} \le m_i \\ \dfrac{med_i - T_i^{-1}}{med_i - m_i}, & m_i < T_i^{-1} < med_i \\ 0, & T_i^{-1} \ge med_i \end{cases} \tag{26}$$

where: $0 < m_p < M_p$, $0 < m_i < M_i$,

$$med_p = \frac{M_p + m_p}{2} \tag{27}$$

$$\frac{1}{med_i} = \frac{1}{2}\left(\frac{1}{m_i} + \frac{1}{M_i}\right) \tag{28}$$

Crisp values of K_p, $1/T_i$ are calculated by the centroid defuzzification method [12]. The FL1SC provides improved performance compared to the PISC [12] but its speed responses contain high undershoot and overshoot. Next paragraph is presentation of PI speed controller with Fuzzy Logic-Based Adaptation and Scheduling Boundaries blocks (FL2SC).

Scheduling Boundaries block is utilized to tune the parameters m_i & M_i of the $1/T_i$ as follows:

$$m_i(t) = \frac{med_i}{1 + f(e_{\omega,n}, t)} \tag{29}$$

$$M_i(t) = \frac{med_i}{1 - f(e_{\omega,n}, t)} \tag{30}$$

where: $0 < f(e_{\omega,n},t) < 1$. For simplicity, the $f(e_{\omega,n},t)$ is assumed to be a linear function according to Eq. (31):

$$f(e_{\omega,n}, t) = \begin{cases} c_k e_{\omega,n} + bw_i, \ for \ t_{1k} \le t \le t_{2k} \\ bw_i, for \ t < t_{1k} \cap t > t_{2k} \end{cases} \tag{31}$$

where: t_{1k}, t_{2k}: times when motor speed respectively moves from inside/outside range ±2% around ω_{ref} to outside/inside this range in duration k of speed response for the FL1SC; c_k is limited in range $\pm bw_i$ and selected experimentally;

$$bw_i = \left(med_i - m_i\right)/m_i \tag{32}$$

Simulation Results

This section simulates three speed controllers including PISC, FL1SC, FL2SC in Simulink environment of Matlab software at ω_{ref} =100rpm and T_L={$0.1T_N$, $0.3T_N$, $0.5T_N$, $0.7T_N$} with PMSM parameters given in Table 1, DC link voltage of 372V, switching frequency of 20kHz. Two limitations of the $T_{e,ref}$ are $\pm T_N$ The PISC has K_p=0.05, T_i=0.02s. Parameters of the FL1SC are B_e=1, $B_{\Delta e}$=0.0015, m_p=0.01, M_p=0.09, m_i=1/0.037, M_i=1/0.003, bw_i=0.85. Figure 2 shows diagrams of reference motor speed and load torque. There are 5 durations and coefficients c_k listed in Table 3. The overshoot/undershoot, settling time, and the integral of time multiply by absolute speed error (*ITAE* in Eq. (33)) are utilized to evaluate the three controllers performance:

$$ITAE = \int_0^1 t\left|e_\omega(t)\right| dt \tag{33}$$

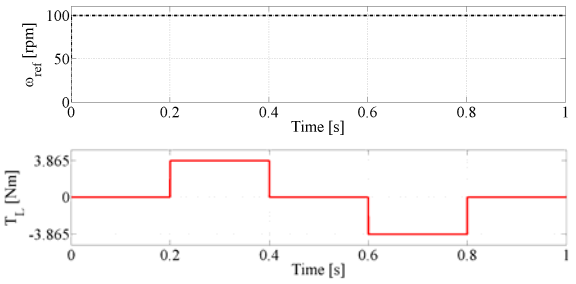

Fig.2. Diagrams of reference motor speed (upper) and load torque at ω_{ref} = 100rpm, $T_L = 0.5T_N$.

Table 3. Coefficient c_k of the FL2SC

Duration				
k =1 (0.0s-0.2s)	k =2 (0.2s-0.4s)	k =3 (0.4s-0.6s)	k =4 (0.6s-0.8s)	k =5 (0.8s-1.0s)
-0.85	0.3	-0.25	-0.3	0.25

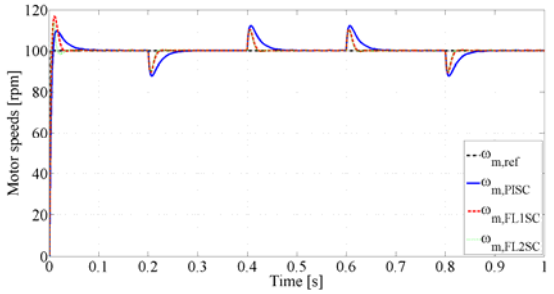

Fig.3. Motor speed responses at $T_L = 0.1T_N$.

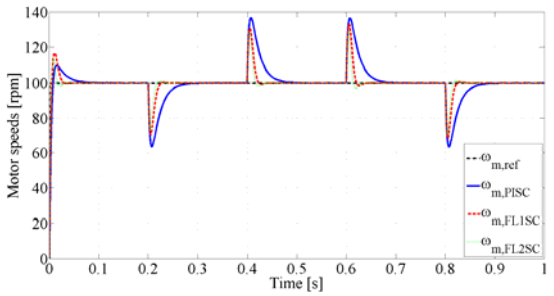

Fig.4. Motor speed responses at $T_L = 0.3T_N$.

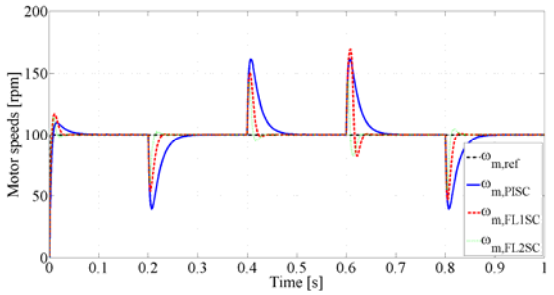

Fig.5. Motor speed responses at $T_L = 0.5T_N$.

Motor speed responses at load torques of $0.1T_N$, $0.3T_N$, $0.5T_N$ & $0.7T_N$ are shown in Figures 3-6, respectively. For duration 1, the PISC brings the minimum overshoot (see Tables 4-7) and longest settling time (see Tables 8-11). Reason for this is the PISC owns smallest K_p and longest T_i at motor starting (see duration 0.0s-0.1s in Figs. 7-10). For durations 2-5, advantage in overshoot/undershoot belongs to the FL2SC. It reduces 15%-44% and 1.9%-84% overshoot/undershoot respectively compared to the PISC and the FL1SC, and the value decreases more as the load torque increases, especially at duration 4 of $T_L = 0.7T_N$ (see Fig. 6). The cause of this problem is the large and sudden change of the load torque leads to a sudden change in the

motor speed, and the motor speed error. In order to lower the $e_{\omega,n}$, the FL1SC tries to reduce the K_p, which results in high deceleration (see Fig. 10). Meanwhile, the FL2SC narrows the boundaries m_i & M_i of inversion of the integral time constant, thereby avoiding sudden K_p reduction. In the Tables 8-11, the FL2SC provides 0.025s-0.046s shorter settling time than PISC. It also brings approximate settling time compared to the FL1SC, except for the case of duration 4 in Fig. 6 with 0.043s shorter settling time.

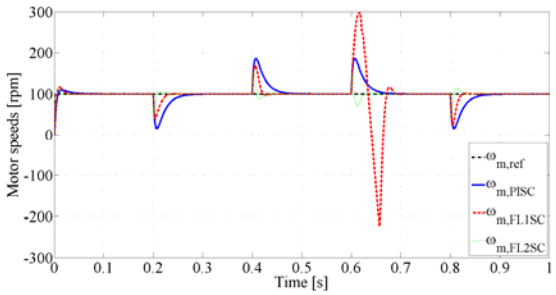

Fig.6. Motor speed responses at $T_L = 0.7T_N$.

Table 4. Overshoot/Undershoot [rpm] at $T_L = 0.1T_N$

Speed controller	Duration				
	1	2	3	4	5
PISC	**9.6**	12.2	12.2	12.2	12.1
FL1SC	16.8	10.3	10.3	10.4	10.5
FL2SC	13.9	**10.1**	**10.1**	**10.2**	**10.3**

Table 5. Overshoot/Undershoot [rpm] at $T_L = 0.3T_N$

Speed controller	Duration				
	1	2	3	4	5
PISC	**9.6**	36.5	36.6	36.6	36.6
FL1SC	16.8	29.7	30.7	33.0	31.5
FL2SC	13.9	**27.3**	**28.5**	**29.2**	**29.1**

Table 6. Overshoot/Undershoot [rpm] at $T_L = 0.5T_N$

Speed controller	Duration				
	1	2	3	4	5
PISC	**9.6**	61.0	61.0	61.0	61.0
FL1SC	16.8	46.5	50.0	69.2	53.4
FL2SC	13.9	**39.9**	**43.0**	**44.2**	**45.3**

Table 7 Overshoot/Undershoot [rpm] at $T_L = 0.7T_N$

Speed controller	Duration				
	1	2	3	4	5
PISC	**9.6**	85.3	85.4	85.4	85.4
FL1SC	16.8	60.9	67.9	323.8	77.4
FL2SC	13.9	**47.8**	**52.9**	**50.4**	**56.7**

Table 8. Settling time [s] at $T_L = 0.1T_N$

Speed controller	Duration				
	1	2	3	4	5
PISC	0.047	0.240	0.442	0.642	0.841
FL1SC	0.024	0.217	0.417	0.617	0.817
FL2SC	**0.015**	**0.215**	**0.415**	**0.615**	**0.815**

Table 12 indicates that the FL2SC gives ITAE value 2.7-5.2 times and 1.1-8.9 less than the PISC and the FL1SC, respectively. Diagrams of stator currents, estimate values of stator flux components and motor torque at $T_L = 0.7T_N$ are presented in Figs. 11-13. The FL2SC provides smoother responses of current and estimate values of flux components than the PISC and the FL1SC (see Figs. 11-12). Torque response of the FL2SC owns lower fluctuation than the FL1SC. It also has higher peaks that last in shorter duration than the PISC and the FL1SC, resulting in a speed response with lower overshoot/undershoot and shorter settling time.

Table 9. Settling time [s] at $T_L = 0.3T_N$

Speed controller	Duration				
	1	2	3	4	5
PISC	0.047	0.258	0.459	0.658	0.859
FL1SC	0.024	0.221	0.420	**0.618**	0.820
FL2SC	**0.015**	**0.215**	**0.415**	0.625	**0.815**

Table 10. Settling time [s] at $T_L = 0.5T_N$

Speed controller	Duration				
	1	2	3	4	5
PISC	0.047	0.267	0.468	0.667	0.866
FL1SC	0.024	0.225	**0.421**	0.634	**0.821**
FL2SC	**0.015**	**0.221**	0.427	**0.626**	0.825

Table 11. Settling time [s] at $T_L = 0.7T_N$

Speed controller	Duration				
	1	2	3	4	5
PISC	0.047	0.272	0.472	0.672	0.873
FL1SC	0.024	0.229	0.431	0.688	**0.822**
FL2SC	**0.015**	**0.224**	**0.428**	**0.625**	0.827

Table 12. ITAE [s^2·rpm]

Speed controller	T_L			
	$0.1T_N$	$0.3T_N$	$0.5T_N$	$0.7T_N$
PISC	0.667	1.951	3.235	4.521
FL1SC	0.270	0.755	1.432	7.724
FL2SC	**0.245**	**0.542**	**0.730**	**0.860**

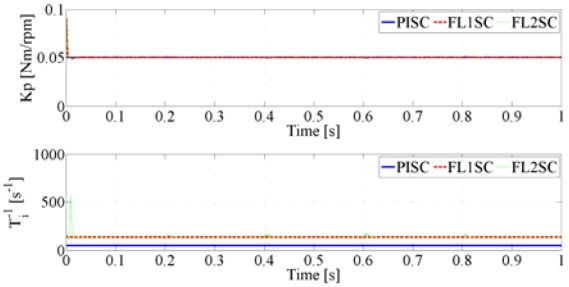

Fig.7. Parameters K_p (upper), $1/T_i$ at $\omega\, T_L = 0.1T_N$.

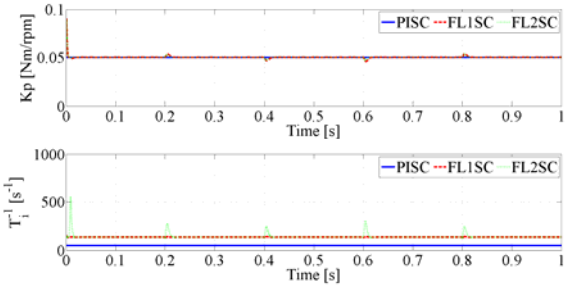

Fig.8. Parameters K_p (upper), $1/T_i$ at $T_L = 0.3T_N$.

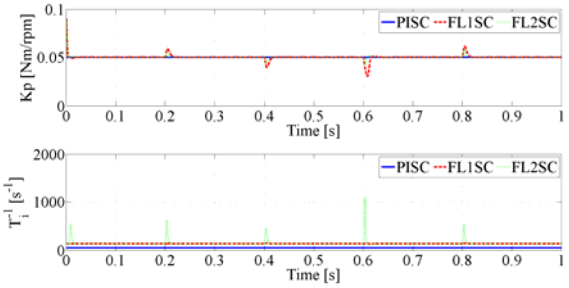

Fig.9. Parameters K_p (upper), $1/T_i$ at $T_L = 0.5T_N$.

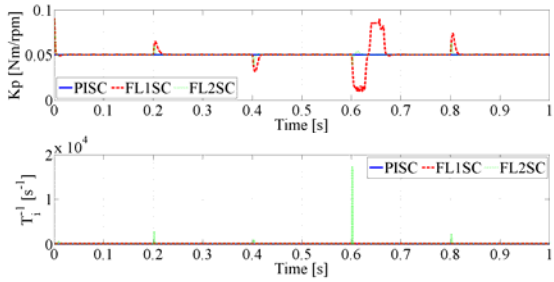

Fig.10. Parameters K_p (upper), $1/T_i$ at $T_L = 0.7T_N$.

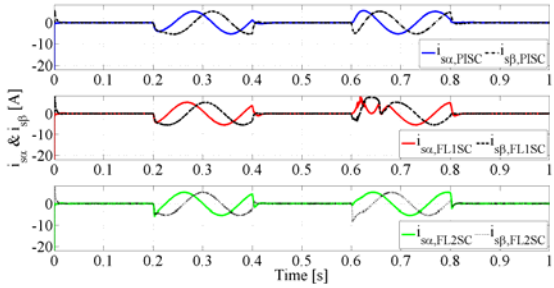

Fig.11. Stator current components at $T_L = 0.7T_N$.

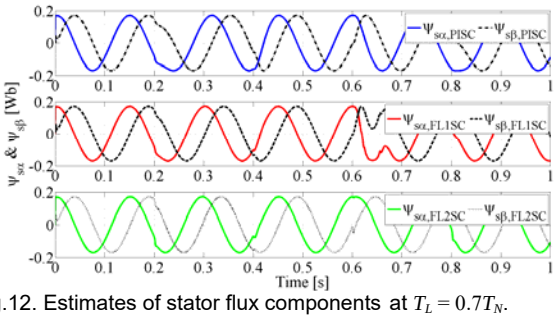

Fig.12. Estimates of stator flux components at $T_L = 0.7T_N$.

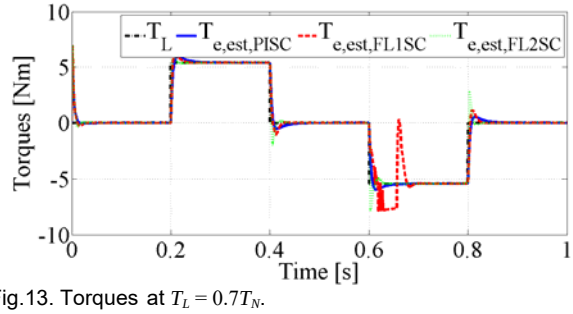

Fig.13. Torques at $T_L = 0.7T_N$.

Conclusions

Drive structure using fuzzy logic PI speed controller with scheduling boundaries of integral constant time as a linear function of speed error was presented. Simulations were implemented at different values of load torques. The proposed speed controller significantly brought lower overshoot/undershoot, shorter settling time, smaller ITAE value for speed response than the conventional PI one and the one without scheduling boundaries. Besides that, it also gave smoother stator current & flux, and faster & more robust motor torque than two other ones. Online methods such as neural networks can be integrated to schedule the boundaries. Type-2 fuzzy controllers can be employed to get better performance. The proposed method can be applied in sensorless control of PMSM drive.

***Authors**: Dr. Hau Huu Vo, Modeling Evolutionary Algorithms Simulation and Artificial Intelligence, Faculty of Electrical and Electronics Engineering, Ton Duc Thang University, No. 19 Nguyen Huu Tho Street, Tan Phong Ward, District 7, Ho Chi Minh City, Vietnam, E-mail: vohuuhau@tdtu.edu.vn*
Prof. Ing. Pavel Brandstetter, VSB-Technical University of Ostrava, Faculty of Electrical Engineering and Computer Science, Department of Electronics, 17.listopadu 15, 70833 Ostrava-Poruba, Czech Republic, E-mail: pavel.brandstetter@vsb.cz.
**Corresponding Author: Hau Huu VO (E-mail: vohuuhau@tdtu.edu.vn)*

REFERENCES

[1] Knypinski L., Krupinski J., Application of the permanent magnet synchronous motors for tower cranes, *Przegląd Elektrotechniczny*, 96 (2020), nr 1, 27-30
[2] Wu G., Huang S., Wu Q., Rong F., Zhang C., Liao W., Robust Predictive Torque Control of N*3-Phase PMSM for High-Power Traction Application, *IEEE Transactions on Power Electronics*, 35 (2020), No. 10, 10799-10809
[3] Gupta U., Yadav D.K., Panchauli D., Field Oriented Control of PMSM during Regenerative Braking, *2019 Global Conference for Advancement in Technology (GCAT)*, Bangalore, India, 2019, 1-5
[4] Kouriche L., Messlem Y., Mras-super twisting sliding mode observer for speed sensorless vector control of induction motor drive, *Przegląd Elektrotechniczny*, 97 (2021), nr 4, 121-127
[5] Vo H.H., Brandstetter P., Tran T.C., Dong C.S.T., An Implementation of Rotor Speed Observer for Sensorless Induction Motor Drive in Case of Machine Parameter Uncertainty, *Advances in Electrical and Electronic Engineering*, 16 (2018), No. 4, 426-434
[6] Harikrishnan R., George A.E., Direct Torque Control of PMSM using hysteresis modulation, PWM and DTC PWM based on PI Control for EV - A comparative analysis between the three strategies, *2019 2nd International Conference on Intelligent Computing, Instrumentation and Control Technologies (ICICICT)*, Kannur, India, 2019, 566-571
[7] Chaoui H., Khayamy M., Okoye O., Gualous H., Simplified Speed Control of Permanent Magnet Synchronous Motors Using Genetic Algorithms, *IEEE Transactions on Power Electronics*, 34 (2019), No. 4, 3563-3574
[8] Rauth S.S., Samanta B., Comparative Analysis of IM/BLDC/PMSM Drives for Electric Vehicle Traction Applications Using ANN-Based FOC, *2020 IEEE 17th India Council International Conference (INDICON)*, New Delhi, India, 2020, 1-8
[9] Gandhi R., Wilson R., Kumar A., Roy R., Comparative Analysis of Vector Controlled PMSM Drive with Particle Swarm Optimization and Ant Colony Optimization Technique, *2020 International Conference on Computational Performance Evaluation (ComPE)*, Shillong, India, 2020, 744-750
[10] Adhavan B., Kuppuswamy A., Jayabaskaran G., Jagannathan V., Field oriented control of Permanent Magnet Synchronous Motor (PMSM) using fuzzy logic controller, *2011 IEEE Recent Advances in Intelligent Computational Systems*, Trivandrum, India, 2011, 587-592
[11] Berkani A., Negad K., Allaoui T., Marignetti F., Fuzzy Direct Torque Control for Induction Motor Sensorless Drive Powered by Five Level Inverter with Reduction Rule Base, *Przegląd Elektrotechniczny*, 95 (2019), nr 7, 66-71
[12] Vo H.H., Kuchar M., Brandstetter P., Application of Fuzzy Logic in Sensorless Induction Motor Drive with PWM-DTC, *Electrical Engineering*, 102 (2020), No. 1, 129-140
[13] Naik N V., Singh S.P., Panda, A.K., An Interval Type-2 Fuzzy-Based DTC of IMD Using Hybrid Duty Ratio Control, *IEEE Trans. on Power Electronics*, 35 (2020), No. 8, 8443-8451
[14] Perdukova D., Fedor P., Lacko M., DC motor fuzzy model based optimal controller, *MM Science Journal*, 14 (2021), Oct 2021, 4879-4885
[15] Brandstetter P., Neborak I., Kuchar M., Analysis of Steady-State Error in Torque Current Component Control of PMSM Drive, *Advances in Electrical and Computer Engineering*, 17 (2017), No. 2, 39-46
[16] Orlowska-Kowalska T., Dybkowski M., Stator-Current-Based MRAS Estimator for a Wide Range Speed-Sensorless Induction-Motor Drive, *IEEE Transactions on Industrial Electronics*, 57 (2010), No. 4, 1296-130